The 2016 World Congress on
Advances in Civil, Environmental, and Materials Research (ACEM16)
Jeju Island, Korea, August 28-September 1, 2016

Tailoring the Magnetic, Dielectric and Structural Properties of Cobalt Doped α-Fe_2O_3 Nanoparticles

*Zaheer H. Shah[1)], Saira Riaz[2)], Zohra N. Kayani[3)] and Shahzad Naseem[4)]

[1), 2), 4)] *Centre of Excellence in Solid State Physics, University of Punjab, Lahore, Pakistan*
[1)] *Department of Physics, UMT, Lahore, Pakistan*
[3)] *Department of Physics, LCWU, Lahore, Pakistan*
[4)] *shahzad.cssp@pu.edu.pk*

ABSTRACT

In this work undoped and cobalt doped α-Fe_2O_3 nanoparticles (NPs) have been synthesized using sol-gel method. Dopant concentration is varied in the range of 2 to 8 wt%. Presence of diffraction peaks corresponding to (104), (110), (024) and (116) indicate the formation of α-Fe_2O_3 phase under as-synthesized conditions. XRD peak positions shift to relatively higher angles as compared to undoped NPs. Such shift in peak position might have been observed because of the lower ionic radius of cobalt (72pm) as compared to iron (74pm). SEM results confirm the formation of NPs with diameter less than 50nm. Undoped and cobalt doped iron oxide NPs show ferromagnetic behavior. Saturation magnetization increases as dopant concentration is increased to 8wt%. Slight decrease in dielectric constant is observed as frequency of applied field increases. However, as frequency of applied field increases to log f [Hz] >6.5 increase in dielectric constant is attributed to resonance effect. Tangent loss exhibits normal dispersion behavior i.e. decreases as frequency of applied field increases and becomes constant in high field region. Decrease in a.c. conductivity with increase in dopant concentration to 6wt% indicates that ionic transport is suppressed with cobalt doping in Fe_2O_3 nanoparticles

1. INTRODUCTION

Metal oxide nanostructures such as SnO_2, In_2O_3, ZnO, TiO_2, CuO, and Fe_2O_3 have reaped much attention due to potential applications in the field of optics, toxic and explosive gas sensing, magnetic recording devices and magnetic resonance imaging (Hao et al. 2015, Peng et al. 2002, Pan et al. 2001). Among all of these metal oxides, iron oxide (α-Fe_2O_3) nanoparticles have been widely investigated because of unique n-type semiconductor nature. α-Fe_2O_3 is stable, low cost and environment friendly phase of iron oxide (Zhou et al. 2014, Riaz et al. 2013). In the family of magnetic materials, α-Fe_2O_3 nanocrystals have antiferromagnetic properties with large amount of commercial

applications in lithium ion batteries, pigments, PEC water splitting and magnetic storage devices (Cesar et al. 2006, Huang et al. 2015).

Therefore, owing to such bundle of applications many techniques have been used to fabricate different shapes of nanoparticles to meet the target quality point. However, the magnetic properties of α-Fe_2O_3 nanoparticles such as coercivity, and saturation magnetization are not still enough to hit the commercial demand of magnetic materials. To quench the thirst of magnetic nanomaterials to some extent doping of transition metals (Si, Ti and Sn) in α-Fe_2O_3 result excellent magnetic properties (Sun et al. 2014, Wang et al. 2011, Riaz et al. 2014a,b, Akbar et al. 2014a,b).

α-Fe_2O_3 nanoparticles have been prepared using different types of experimental techniques like hydro thermal, force hydrolysis, precipitation and solvo thermal method (Wen et al. 2005, Jagadeesan et al. 2008). Recently, many material scientists have regulated α-Fe_2O_3 morphology and structures using supra-molecular, surfactant and micelles to obtain particular structured hematite nano materials. For example the nano cubic hematite polyhedrons have been synthesized by hydrothermal method in the presence of CH_3COO^-, to control the shape and size of particles (Zhang et al. 2010). Furthermore, single crystal α-Fe_2O_3 hexagonal nano rings with hexagonal inner holes have been synthesized under the stepwise influence of various kinds of anionic ligands (Zhang et al. 2010, Su et al. 2011). In the present work, wet chemical sol-gel route has been utilized to fabricate mono dispersed Co-doped α-Fe_2O_3 and have been investigated for their magnetic and dielectric properties. The sol-gel method has been found most efficient, low cost and environment friendly (Riaz et al. 2014a,b, Akbar et al. 2015). The nanoparticles prepared by this method are well shaped and homogeneously distributed.

The focus of this study is to examine magnetic, dielectric and structural properties of Co-doped α-Fe_2O_3 nanocrystals. The synthesized α-Fe_2O_3 nanostructures in the present study have potential applications in many fields and fulfill the challenges of the research world.

2. EXPERIMENTAL DETAILS

Doped α-Fe_2O_3 nanoparticles were synthesized via sol gel method. The stoichiometric amount of starting materials was weighed using electronic balance. The homogeneous mixture of precursors was made in deionized water (DI). The solution was put on the hot plate and transferred into the ESCO fume hood. The solution was heated in definite interval of temperature which led to a sol formation. The sol was heated to obtain gel and eventually powder.

Further, different characterization techniques were used to study the various properties of as synthesized nanoparticles. The crystal size and structure of samples was investigated by Bruker D8 Advance X-ray diffractometer (XRD) with CuK_α (1.5406Å) radiations. Lake Shore's 7407 vibrating sample magnetometer (VSM) examined the magnetic properties. Dielectric properties were analyzed with the help of 6500 Precision impedance analyzer.

3. RESULTS AND DISCUSSION

Figure 1 exhibits the X-ray diffraction (XRD) pattern of as synthesized Co-doped α-Fe_2O_3 sample in the 2θ range of 20-80° under the Cu-K_α radiation (λ = 1.5406Å). Indexing of obtained pattern was performed according to the procedure as explained by Cullity (1975). The most prominent peaks (104), (110), (024) and (116) revealed that Co-doped α-Fe_2O_3 has hexagonal crystal structure. The results show that cobalt is successfully substituted in the α-Fe_2O_3 without disturbing the hexagonal crystal structure and there is no impurity peak which proves that phase pure Co-doped α-Fe_2O_3 nano structures have been obtained. It can be seen from the XRD pattern in Fig.1 that as doping concentration was increased from 4wt% to 8wt%, the indexed peaks are shifted towards higher angle, such shifting occurs due to the difference between ionic radius of Co^{2+} (72 pm) and Fe^{3+} (74 pm) ions. This difference in ionic radius leads to decrease in unit cell volume and lattice parameters (Table 1). This according to Bragg's Law shifts the peak positions to higher angles.

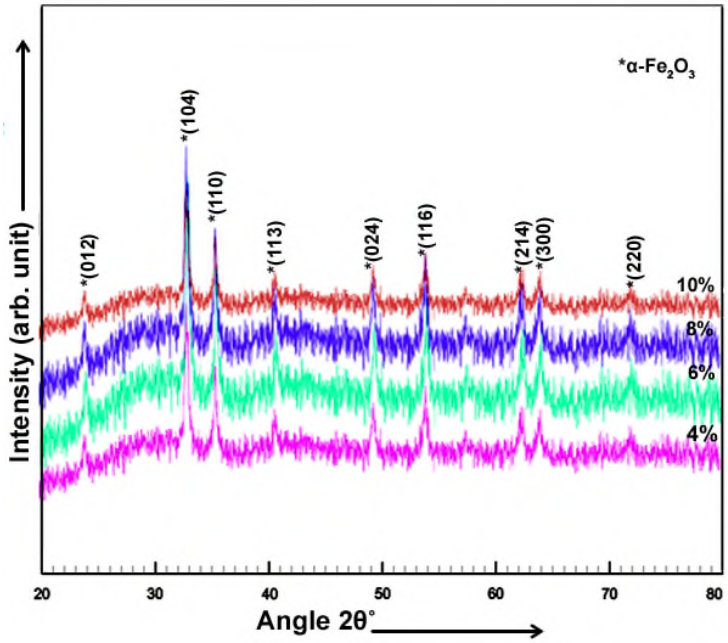

Fig. 1 XRD patterns for Co doped α-Fe_2O_3 nanoparticles

Table 1 Lattice parameters and unit cell volume for Co doped α-Fe_2O_3 nanoparticles

Dopant concentration (%)	Lattice parameters (Å)		Unit cell volume ($Å^3$)
	a	c	
4	5.036	13.752	302.0336
6	5.033	13.749	301.6080
8	5.028	13.701	299.9582
10	5.014	13.604	296.1783

Crystallite size (Cullity 1956) and dislocation density (δ) (Kumar et al. 2011) were determined using Eqs. 1-2

$$t = \frac{0.9\lambda}{B\cos\theta} \quad (1)$$

$$\delta = \frac{1}{t^2} \quad (2)$$

Where, θ represents the diffraction angle, λ is wavelength and B is Full Width at Half Maximum. Crystallite size (Fig. 2) shows increase with 4wt% to 8wt% dopant concentration. This increase in crystallite size and decrease in dislocation density points out that dopant atoms are entirely included in the lattice. At high dopant concentration (10%) decrease in crystallite size and increase in dislocation density point out that dopant atoms have taken the interstitial positions. This directed to decrease in crystalline order and increase in dislocation density (Riaz et al. 2014a,b).

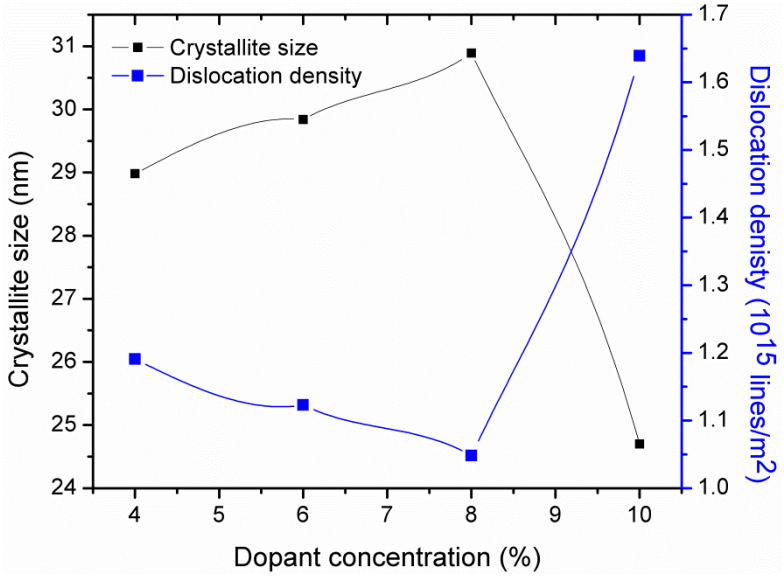

Fig. 2 Crystallite size and dislocation density for Co doped α-Fe_2O_3 nanoparticles

Dielectric constant and tangent loss were calculated using Eqs. 3 and 4 (Barsoukov and Macdonald 2005)

$$\varepsilon = \frac{Cd}{\varepsilon_o A} \quad (3)$$

$$\tan\delta = \frac{1}{2\pi f \varepsilon_o \varepsilon \rho} \quad (4)$$

Where, *C* is the capacitance of films, d is the film thickness, ε_o is the permittivity of free space, A is the area, *f* is the frequency and *ρ* is the resistivity. All these measurements were taken at room temperature in the frequency range of 1kHz-20 MHz (Fig. 3). Initially, decrease in dielectric constant is observed with increase in frequency. This behavior is almost same for all prepared samples. This slight decrease in dielectric constant is associated with hopping of electrons between Fe^{3+} and Fe^{2+}, Co^{3+} and Co^{2+} pairs of ions. Koop's theory is an important tool to explain this decrease in dielectric constant. According to Koop's theory, dielectric materials may be considered as conducting grains which are separated by grain boundaries that are non-conducting (Riaz et al. 2015, Barsoukov and Macdonald 2005). Low value of dielectric constant shows that conducting grains are more active than grains boundaries in the frequency range of 1kHz to 1MHz. At higher frequencies the resistance of grain boundaries increases and electrons start to pile up there which causes polarization and hence the dielectric constant increases (Barsoukov and Macdonald 2005). Increase in dielectric constant at high frequencies is also due to matching of jumping frequency of ions with that of externally applied field. In addition, because of the presence of lattice defects high tangent loss is observed at low frequencies. But as frequency increases these lattice defects are not able to cope with the changes in frequency of the field. Thus tangent loss decreases (Barsoukov and Macdonald 2005). Dielectric constant increased to 375 (log f = 7.3) and tangent loss decreased (Fig. 3) as dopant concentration was increased to 8%. Increase in dielectric constant and decrease in tangent loss is attributed to decrease in lattice defects. This decrease in lattice defects is indicated by decrease in dislocation density and increase in crystallite size (Barsoukov and Macdonald 2005).

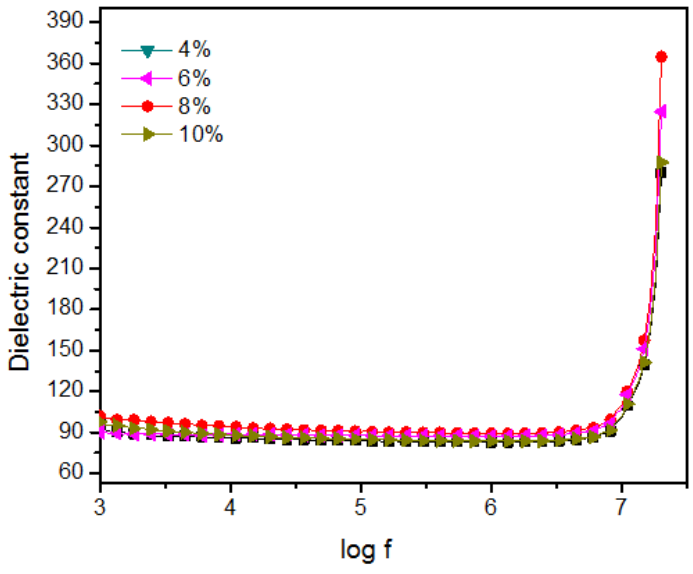

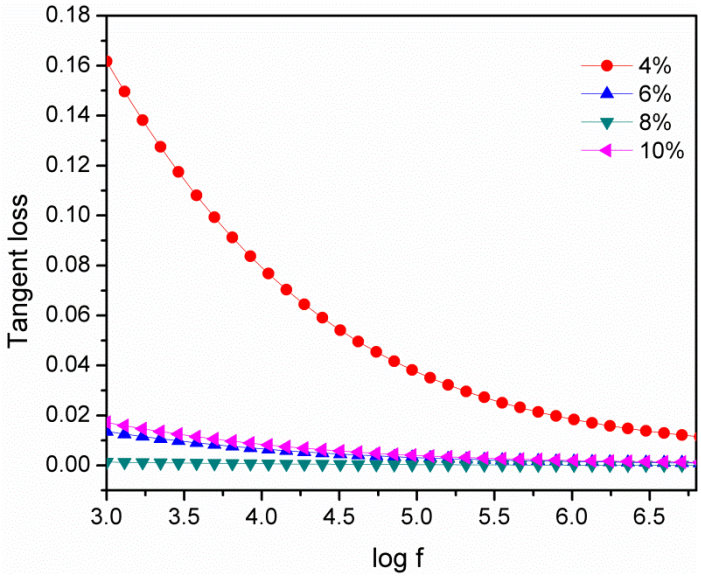

Fig. 3 Dielectric constant and tangent loss plotted for Co doped α-Fe_2O_3 nanoparticles

Conductivity (σ) of Co doped α-Fe_2O_3 nanoparticles was calculated using Eq. 5 (Barsoukov and Macdonald 2005).

$$\sigma = 2\pi f \varepsilon \varepsilon_o \tan\delta \tag{5}$$

Conductivity (Fig. 4) remains constant in low frequency region. This frequency independent region in dielectric material arises due to presence of free charge carriers. The rise in conductivity at high frequencies is due to bound charge carriers that hop from one potential well to another. High frequencies support this hopping process. Presence of both frequency dependent and independent regions indicate that both a.c. and d.c. conductivities contribute to conduction in Co doped iron oxide nanoparticles. Decrease in conductivity with increase in dopant concentration thus indicates that ionic transport is suppressed with cobalt doping in Fe_2O_3 nanoparticles (Shinde et al. 2011, Barsoukov and Macdonald 2005).

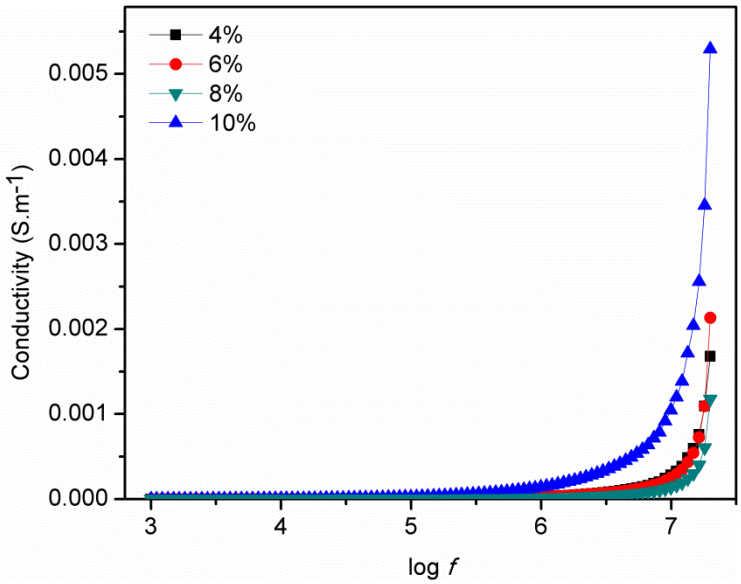

Fig. 4 Conductivity of Co doped α-Fe_2O_3 nanoparticles

M-H cures for Co doped α-Fe_2O_3 can be seen in Fig. 5. α-Fe_2O_3 shows ferromagnetic behavior. In α-Fe_2O_3, spins in same and adjoining planes are ferromagnetically and antiferromagnetically coupled. Because of spin orbit interaction among the planes uncompensated magnetic moments exists. These uncompensated magnetic moments lead to ferromagnetic behavior of α-Fe_2O_3. Further adding, cobalt atom donates one d electron and two s electrons to oxygen anion. As cobalt substitutes iron presence of uncompensated spins leads to increase in magnetization (Riaz et al. 2014a, Akbar et al. 2014b).

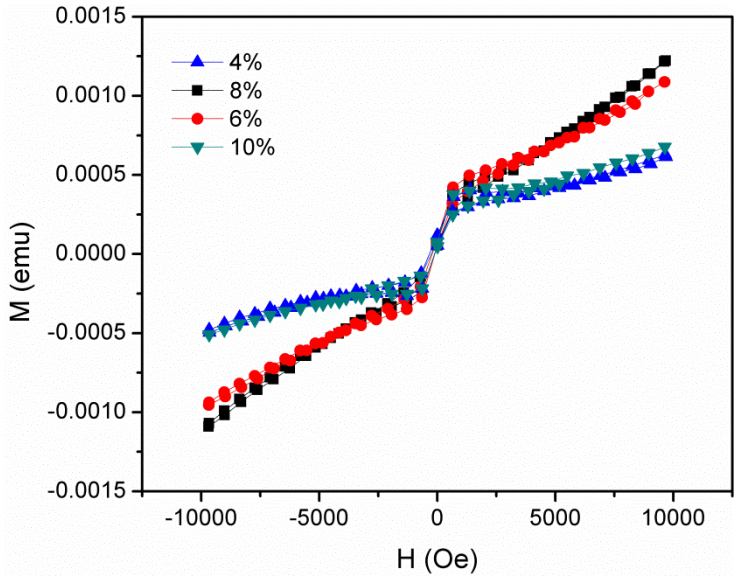

Fig. 5 M-H curves for Co doped α-Fe_2O_3 nanoparticles

4. CONCLUSIONS

Cobalt doped α-Fe_2O_3 nanoparticles were synthesized via sol-gel method. Dopant concentration was kept as 4-10%. XRD results indicated the formation of phase pure α-Fe_2O_3. Increase in crystallite size was observed as dopant concentration was increased to 8%. Dielectric constant showed anomalous dispersion behavior while normal dispersion behavior was observed for tangent loss. Dielectric constant increased to 375 (log f = 7.3) as dopant concentration was increased to 8%. Co doped α-Fe_2O_3 nanoparticles showed ferromagnetic behavior due to presence of uncompensated spins as Co replaced Fe in the host lattice.

REFERENCES

Akbar, A., Riaz, S., Ashraf, R. and Naseem, S. (2014(b)), "Magnetic and magnetization properties of Co-doped Fe_2O_3 thin films," *IEEE Trans. Magn.*, **50**, 2201204

Akbar, A., Riaz, S., Bashir, M. and Naseem, S. (2014a), "Effect of Fe^{3+}/Fe^{2+} Ratio on Superparamagnetic Behavior of Spin Coated Iron Oxide Thin Films," *IEE Trans. Magn.*, **50**, 2200804.

Cesar, I. Kay, A. Martinez, J. A. G. and Grätzel, M. (2006), "Translucent thin film Fe_2O_3 photo anodes for efficient water splitting by sunlight: nanostructure-directing effect of Si-doping." *J. Am. Chem. Soc.* Vol. **128**(14), 4582-4583.

Cullity, B.D. (1956), "Elements of x-ray diffraction," Addison Wesley Publishing Company, USA.

Hao, J. S. Yali, S. and Xiao, H. J. (2015), "Hydrothermal synthesis, growth mechanism and gas sensing properties of Zn-doped α-Fe_2O_3microcubes." *CERAM. INT*., Vol. **41**(4), 13224–13231.

Huang, M. C. Chang, W. S. Lin. J. C. Chang, Y. H. and Wu, C. C. (2015), "Magnetron sputtering process of carbon-doped a-Fe_2O_3 thin films for photo electrochemical water splitting." *J. ALLOY. COMPD.* Vol. **636**, 176-182.

Jagadeesan, D. Mansoori, U. Mandal, P. Sundaresan, A. andEswaramoorthy, M. (2008), "Hollow Spheres to Nanocups: Tuning the Morphology and Magnetic Properties of Single Crystalline α Fe_2O_3 Nanostructures." *Angew. Chem. Int. Ed.* Vol.**47**, 7685 – 7688.

Kumar, N., Sharma, V., Parihar, U., Sachdeva, R., Padha, N. and Panchal, C.J. (2011) "Structure, optical and electrical characterization of tin selenide thin films deposited at room temperature using thermal evaporation method," *J. Nano- Electron. Phys.*, **3**, 117-126

Pan, Z. W. Dai, Z. R. and Wang, Z. L. (2001), "Nanobelts of semiconducting oxides." *Sci.***291**(5510), 1947-1949.

Peng, Z.A. and Peng, X. G. (2002), "Nearly monodisperse and shape-controlled CdSe nanocrystals via alternative routes: nucleation and growth." *J. Am. Chem.*Vol. **124**(13), 3343-3353.

Riaz, S., Akbar, A. and Naseem, S. (2013), "Structural, electrical and magnetic properties of iron oxide thin films," *Adv. Sci. Lett.*, **19**, 828-833.

Riaz, S., Akbar, A. and Naseem, S. (2014a), "Ferromagnetic Effects in Cr-Doped Fe_2O_3 Thin Films," *IEEE Trans. Magn.*, **50**, 2200704

Riaz, S., Ashraf, R., Akbar, A. and Naseem, S. (2014b), "Free Growth of Iron Oxide Nanostructures by Sol-Gel Spin Coating Technique—Structural and Magnetic Properties," *IEE Trans. Magn.*, **50**, 2301805.

Riaz, S., Shah, S.M.H., Akbar, A., Atiq, S., Naseem, S. (2015), "Effect of Mn doping on structural, dielectric and magnetic properties of $BiFeO_3$ thin films," *J. Sol-Gel Sci. Technol.*, **74**, 329-339

Shinde, S.S., Bhosale, C.H. and Rajpure, K.Y. (2011), "Studies on morphological and electrical properties of Al incorporated combusted iron oxide," *J. Alloy Compd.*, **509**, 3943–3951.

Su, C. H. Wang, H. and Liu, X. J. (2011), "Controllable fabrication and growth mechanism of hematite cubes." *Cryst. Res. Technol.* Vol. **2**, 209–214.

Sun, P. Wang, C. Zhou, X. Cheng, P. Shimanoe, K. Lu, G. and Yamazoe, N. (2014), "Cu-doped -Fe_2O_3 hierarchical microcubes: Synthesis and gas sensing properties." *SENSOR. ACTUAT. B.* Vol. **193**, 616-622.

Wang, G. Ling, Y. Wheeler, D. A. George, K. E. N. Horsley, K. Heske, C. Zhang, J. Z. and Li, Y. (2011) "Facile synthesis of highly photoactive α-Fe_2O_3-based films for water oxidation." *Nano. Lett.* Vol. **11**(8), 3503-3509.

Wen, X. Wang, S. Ding, Y. Wang, Z. L. and Yang, S. (2005), "Controlled Growth of Large-Area, Uniform, Vertically Aligned Arrays of α Fe_2O_3 Nanobelts and Nanowires."*J. Phys. Chem. B*. Vol. **109**(1), 215–220.

Zhang, J. Thurber, A. Hanna, C. and Punnoose, A. (2010), "Highly Shape-Selective Synthesis, Silica Coating, Self-Assembly, and Magnetic Hydrogen Sensing of Hematite Nanoparticles." *LANGMUIR.* Vol. **26**(7), 5273–5278.

Zhou, X. Wang, C. Feng, W. Sun, P. Li, X. W. and Lu, G. Y. (2014), "Hollow α-Fe_2O_3 quasi-cubic structures: hydrothermal synthesis and gas sensing properties." *Mater. Lett.* Vol.**120**, 5–8.